land

MDPI

Review

Geoinformation Technology in Support of Arctic Coastal Properties Characterization: State of the Art, Challenges, and Future Outlook

George P. Petropoulos *, Triantafyllia Petsini and Spyridon E. Detsikas

Department of Geography, Harokopio University of Athens, El. Venizelou St., 70, 17671 Athens, Greece; gp223109@hua.gr (T.P.); sdetsikas@hua.gr (S.E.D.)
* Correspondence: gpetropoulos@hua.gr; Tel.: +30-2109549163

Abstract: Climate change is increasingly affecting components of the terrestrial cryosphere with its adverse impacts in the Arctic regions of our planet are already well documented. In this context, it is regarded today as a key scientific priority to develop methodologies and operational tools that can assist towards advancing our monitoring capabilities and improving our decision-making competences in Arctic regions. In particular, the Arctic coasts are the focal point in this respect, due to their strong connection to the physical environment, society, and the economy in such areas. Geoinformation, namely Earth Observation (EO) and Geographical Information Systems (GISs), provide the way forward towards achieving this goal. The present review, which to our knowledge is the first of its kind, aims at delivering a critical consideration of the state-of-the-art approaches exploiting EO datasets and GIS for mapping the Arctic coasts properties. It also furnishes a reflective discussion on the scientific gaps and challenges that exist that require the attention of the scientific and wider community to allow exploitation of the full potential of EO/GIS technologies in this domain. As such, the present study also serves as a valuable contribution towards pinpointing directions for the design of effective policies and decision-making strategies that will promote environmental sustainability in the Arctic regions.

Keywords: shoreline mapping; coastal erosion; remote sensing; GIS; Arctic; coastal vulnerability

Citation: Petropoulos, G.P.; Petsini, T.; Detsikas, S.E. Geoinformation Technology in Support of Arctic Coastal Properties Characterization: State of the Art, Challenges, and Future Outlook. *Land* **2024**, *13*, 776. https://doi.org/10.3390/land13060776

Academic Editor: Augusto Pérez-Alberti

Received: 4 April 2024
Revised: 16 May 2024
Accepted: 27 May 2024
Published: 30 May 2024

1. Introduction

Human and natural ecosystems are significantly affected by global climate change with coastal zones being heavily impacted [1]. Coastal zones play a critical role in many economies, as they support a variety of social and economic activities and are the link between the terrestrial and marine environments [2]. At the local scale, coastlines are subject to change due to several factors, which are due to political, economic, social, environmental, and climatic parameters [3]. A coastline is defined as the line separating the mainland from the ocean and is one of the most basic features on a topographical map [4,5]. As global temperatures rise and ice melts, sea levels are rising, posing significant threats to coastal communities worldwide (Figure 1). Rising sea levels exacerbate coastal erosion, flooding is localized in high altitude areas, and the impacts on storm surges and flooding are amplified. Arctic temperatures are rising rapidly relative to the global average, which affects Arctic environments that are vulnerable to global warming [6]. Permafrost is the main phenomenon found in the Arctic; it is increasingly influenced by climate change [7]. In recent decades, permafrost has been characterized by high percentages of erosion on Arctic shorelines [8]. Warming is the main factor leading to high rates of coastal erosion [9]. Other factors that play an important role are the anthropogenic impacts of the construction of infrastructure in the coastal areas of the Arctic zone. The intense and high waves, the intense storms, and the increasing duration of the open sea season are some other factors that contribute to erodibility [10].

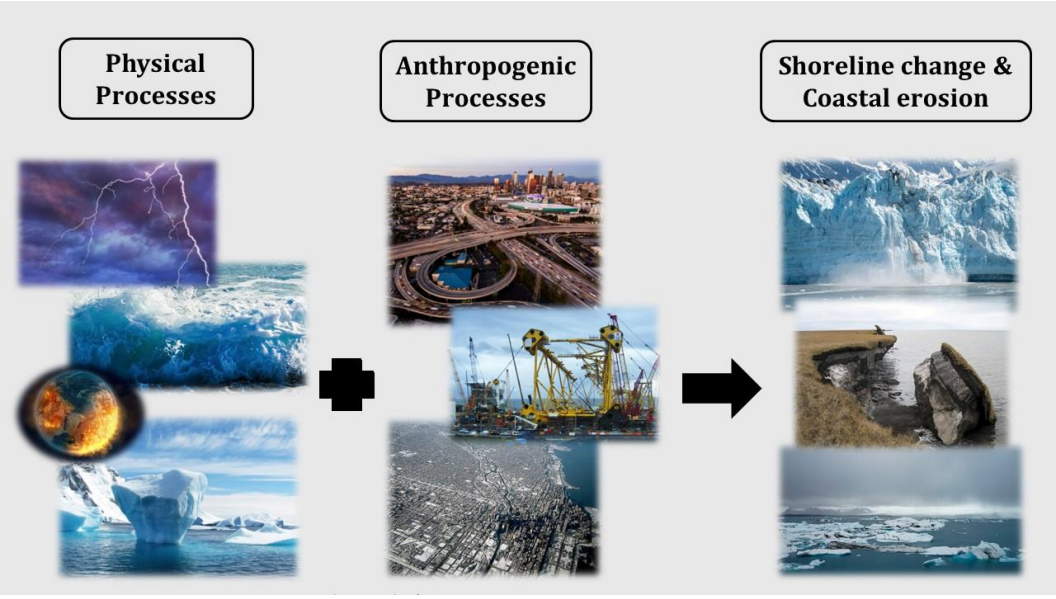

Figure 1. Illustration showing the main contributing factors to shoreline change and coastal erosion in the Arctic region (credit: authors).

In recent years, most of the world's population has been situated near tidal estuaries and coastlines [11]. One third of the Earth's coastlines are affected by permafrost areas [12]. Because of rapid economic development, the natural environment of coastal areas has changed dramatically [13]. Therefore, it is quite important to explore the coastal changes in the Arctic zone [14].

On a global scale, a wide range of studies have been carried out that examine coastal properties and the vulnerability of coastlines [15–17]. As it is challenging to obtain long-term continuous ground-based observations due to the harsh weather in the Arctic, observations from space using Earth Observation (EO) satellites are required to investigate the inner connections between Arctic dynamics and climate change impacts on society and the economy. EO is increasingly used to monitor and detect coastlines as well as establish the degree of vulnerability, with many relevant studies identified in the relevant literature, e.g., [7,17–19]. Furthermore, Geographical Information Systems (GISs) can capture, display, integrate, and analyze a large number of geospatial data, which explains their often-synergistic use with EO datasets [20–22].

The present review aims at providing a critical reflection on the state-of-the-art approaches exploiting EO and GIS for mapping coastal properties in the Arctic regions, focusing on coastal mapping, erosion, and shoreline vulnerability. It also delivers a discussion on the scientific gaps and challenges that require the attention of the scientific and wider community to exploit the full potential of EO/GIS in this domain. As such, this review, which to our knowledge is the first of it is kind, can also provide a useful contribution towards pinpointing directions for designing effective policies and decision-making strategies that will help ensure a more sustainable environment in the Arctic regions.

2. Overall Methodological Approach

In the framework of this literature review, an online search of peer-reviewed international journals was conducted. The international academic database "Scopus" was used as a tool for the present search to extract all the relevant literature on the use of EO/GIS technologies in mapping coastal properties in the Arctic.

In line with previous similar studies [23–25], the search strategy included the following steps. The first step is that of "Identification", where an initial exploration was carried out using a set of specific keywords. A search of the relevant literature was conducted based on the different processes (coastal extraction and erosion and coastal vulnerability)

that characterize coastal management and analysis of the Arctic regions using Earth observation. The Boolean operators used to search the database are as follows: ("remote sensing" AND "coastline" AND "Arctic") OR ("remote sensing" AND "shoreline change" AND "Arctic") OR ("remote sensing" AND "coastal erosion" AND "Arctic"). From the search, 97 documents were extracted. The next step is "Screening", allowing the results to be narrowed down. The criteria set were related to the type of language and types of documents. Thus, documents were extracted that were written only in the English language and consisted of journal articles and book chapters. In addition, a further check was carried out by examining the titles and abstracts of the selected articles to remove those that were not relevant to the topic under investigation. As a result, 25 scientific articles were identified and extracted, covering the period from 2008 to 2024, with their distribution per year illustrated below (Figure 2).

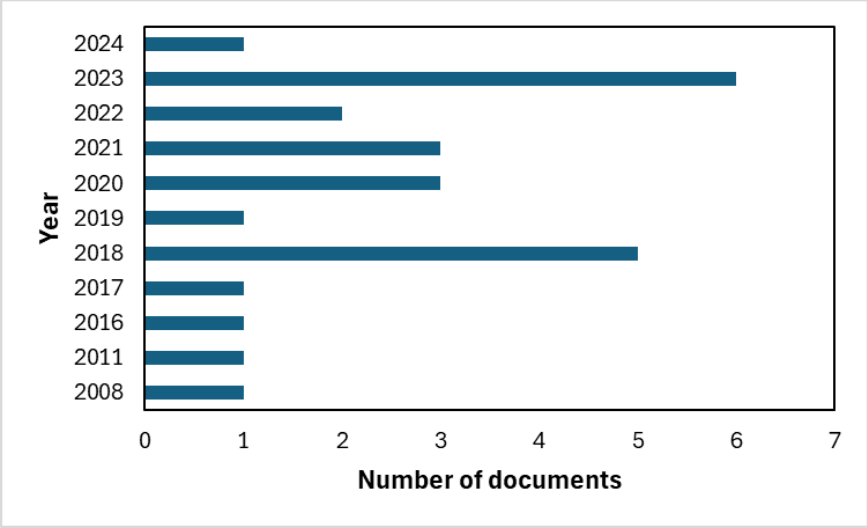

Figure 2. The distribution of published articles examined, spanning from 2008 to 2024.

The extracted results were scientific articles published by high-impact publishers such as MDPI, Taylor and Francis, Elsevier, and Springer. The last step of the methodology is the "Eligibility" phase, where articles were exported to a ".csv" file. The list of articles was viewed in an "Excel" file, and thus the studies were sorted into categories and subcategories based on the coastal management processes investigated in each article and available in the international literature. Figure 3 shows a diagram of the above procedure.

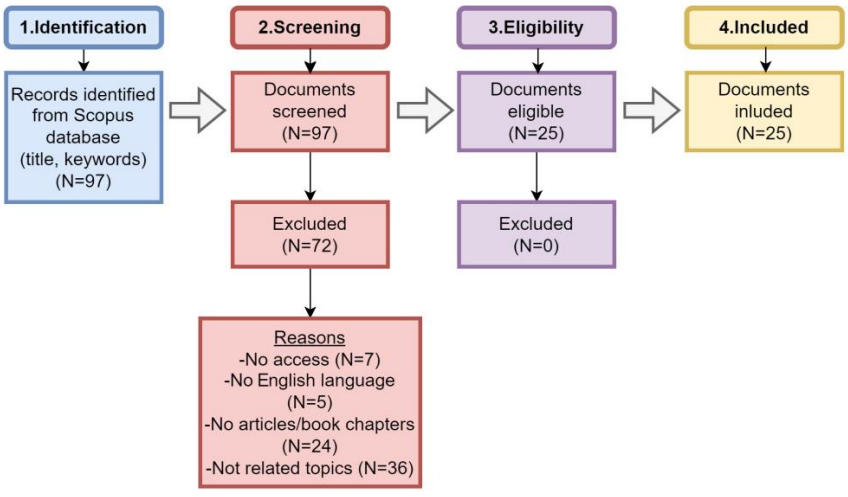

Figure 3. Graphical illustration of methodological approach employed to the literature review study.

3. Coastal Management Approaches for Earth Observation in Arctic Area

This section reviews the studies exploiting EO/GIS technology in extracting coastal properties in the Arctic. It is divided into sections that aim to cover the different thematic areas, providing a concise and reflective description of the different studies and the conclusions that can be drawn in each case.

3.1. Approaches for Coastline Extraction in Arctic Regions

Shoreline changes take place at different spatial scales, ranging from small to larger geographical scales [17]. These changes are affected by various factors and physical processes such as wave height, sediment transport, and sea level rise (SLR). Moreover, e coastal zone changes are highly dependent oncoast morphology, which can be influenced by deposition or erosion [26].

Monitoring coastline position using remote sensing is considered by the remote sensing community nowadays a simple process, but it can be challenging as it sometimes characterized by high uncertainties while there has been observed also low availability in suitable data for analysis. The first attempts to extract and analyze the shoreline used photogrammetric methods, specifically during the period of aerial photography evolution [13,27,28]. This method had high accuracy, but it is time and labor intensive limitng its potential to be used in large geographical scales.

Today, shoreline extraction methods using EO/GIS technologies are divided into two main categories (e.g., see recent review by [17]: (i) manual visual interpretation and (ii) automatic computer-assisted interpretation. On the one hand, manual visual interpretation is characterized by high accuracy and noise resistance, especially in complex areas, while it also enables the continuous extraction of shorelines. On the other hand, the main advantage of automatic computer interpretation is the high efficiency and reusability of the methods due to the automated process. Table 1 presents the methods and subcategories that have been used for shoreline extraction using EO/GIS, specifically in studies conducted in the Arctic region.

Table 1. Overview of the type of methods used to extract coastlines using EO data in the Arctic region.

Methods	Advantages	Disadvantages	Datasets	Examples of Studies
Manual visual interpretation	High accuracy in complex areas	Costly and time-consuming process	Aerial photography, satellite images, SAR images, GPS and DGPS measurements and UAV data	[29–31]
Automated computer-assisted interpretation	Time and cost efficient, high accuracy and reusability of the methods, rapid mapping for large-scale areas, good spatial resolution	Reduced accuracy, it does not consider the tidal effects	Aerial photography, satellite images, Airborne LIDAR	[10,32,33]

3.1.1. Manual Visual Interpretation

Manual visual interpretation is the simplest method used for the extraction of coastlines. In this method, the position of the coastline is determined either by data obtained from aerial photographs or by field survey using data obtained from Global Positioning System (GPS). This method has been implemented repeatedly in numerous studies for different regions worldwide [13,28,34]. Amongst the most frequently used software used to analyze the shoreline position is DSAS tool (version 6) which is further analyzed later in this study (Section 3.3.1).

The authors of [35] used orthorectified aerial photographs and satellite images to extract a coastline through photogrammetric tools to determine coastal erosion. Thus, a semi-automatic method was used. This method calculated the shoreline values manually;

then, the measurement locations for estimating the erosion rate were automatically defined using the DSAS tool. The study area was Herschel Island in Canada. As a result of this study, average erosion rates were obtained over the area, with the largest coastal retreat being identified in the northwestern part of the island, as this area was the most affected by the waves. The accuracy of measurements was calculated using the Dilution of Accuracy (DOA) fraction, having calculated the Root Mean Square Error (RMSE).

Ref. [36] analyzed the dynamics of coastal zone changes in Svalbard, Norway, for the period 1936–2007. Shoreline mapping was manually performed from archived map data and GPS measurements. The influence of a variety of morphogenetic factors was also studied. Over the years, the shoreline was found to have retreated, probably due to the presence of sediments. In another study, ref. [37] used the DSAS tool to extract the shoreline in the Longyearbyen area, Norway. It was implemented with field data and aerial images. The NSM technique was used to calculate shoreline erosion and accretion values for the period 1990–2009. The results showed that intense erosion was observed east of the Longyearbyen delta, where anthropogenic-transformed rock sections were present.

Ref. [9] used manual visual interpretation to map the shoreline at Drew Point, Alaska, to observe changes in coastal erosion between 2008 and 2017. Numerous satellite images were retrieved (Quickbird, IKONOS, GeoEye-1, and Worldview-1 and -2). The DSAS tool measured shoreline changes due to erosion. The analysis showed that erosion increased significantly compared to other studies of previous years. In the same year, ref. [14] used satellite (WorldView-2) and aerial images to estimate shoreline changes at two distinctive geomorphological locations in Alaska between 1950 and 2014. The shoreline was mapped using the manual method, and the DSAS tool was used to calculate erosion rates. At both sites, changes were characterized by high spatial variability in coastal geomorphology.

Ref. [38] investigated the coastal changes of the Yukon Territory coast in Canada. For the study, they used aerial and satellite (GeoEye-1 and WorldView-2) images for the time between 1951 and 2011. They also used differential global positioning system (DGPS) measurements. The manual method led to the mapping of the shoreline; then, by using the DSAS tool and the End Point Rate (EPR) index, coastal erosion was calculated. A decrease in erosion oriented the coastline in a west to east direction. In general, the shoreline retreat rate showed fluctuations over time intervals. The indicator of accuracy, known as DOA, was used to validate this study.

Ref. [29] studied the coastal dynamics of two areas of Baydaratskaya Bay in the Kara Sea and Ural and Yamal coasts in Russia. Satellite (Corona KH-4, QuickBird-2, and WorldView-2, and -3) and aerial images were used as data for estimating the influence of the ongoing coastal erosion processes in the two areas at different time periods. In this scope, shoreline extraction was implemented for each area using direct photointerpretation coupled with the DSAS add on tool in ArcGIS software 10.2 to calculate the erosion rates. In this study, validation was calculated by applying the method of [39] using several sources of uncertainties, such as spatial resolution of the imagery, relative georeferencing of two datasets to each other, and topography-induced horizontal displacement. The results depicted that the Ural coast is eroding at a higher rate compared to the Yamal coast. The authors attribute this to the increased exposure to open sea waves, the more complex lithology of the area, and the high ice content covering the Ural coast.

In another study conducted a few years later, ref. [40] assessed coastal erosion using Synthetic Aperture Radar (SAR) data for three different coasts in Russia. First, the shorelines were mapped using a manual method with a land cover file, and then erosion rates were calculated using the DSAS tool. The results of the study showed that all sites are characterized by high erosion rates. In the same year, ref. [30] calculated long-term observations in the Varendey region of the Barents Sea in Russia. Historical data, field measurements, and Earth observation data (Worldview and GeoEye) were used. The shoreline was manually delineated and divided into three geographic sectors to calculate coastal erosion. The DSAS tool established the erosion rate for the area, with several variations as per the different geographic sectors. In general, in the whole study area, the erosion rates

were highly increased due to extreme weather conditions and fluctuations in environmental factors.

Ref. [41] examined the coastal morphodynamics of the Calypsostranda coast, Svalbard, Norway, for the years 2007–2017, in comparison with previous time intervals (1936–2007) as studied in [36]. The data used were DGPS data, orthophotomaps, and satellite images. Manual shoreline delineation was performed, and EPR and Long RR indices were applied to detect short-term changes. During the two study periods, the shoreline pattern appeared similar, but in the coastal section, erosion was estimated to be greater for the recent period. The authors attributed this to the change in temperature, which had also led to extreme weather events, such as storms.

More recently, ref. [42] analyzed shoreline changes in the Svalbard region, Norway, over 93 years (1927–2020), which consequently had affected coastal cultural heritage sites. Orthophotos, drone images, terrestrial laser scanning (TLS), and topographic surveys were used for the analysis. Manual mapping of the shoreline was performed; then, the DSAS tool was used to assess short- and long-term shoreline erosion. From the analysis, it was observed that the erosion increased due to a new marine formation created in the coastal zone. As a result, the study estimated that many cultural heritage sites located in the circumpolar Arctic will be under risk in the next few decades, which indicates the grave danger of the Arctic's overall cultural heritage if local authorities do not act accordingly.

Ref. [43] investigated for the first time the coastal dynamics of the Kara Sea in Russia using UAV data. This data was used to create images and a Digital Elevation Model (DEM). The analysis was implemented with UAVs, DGPS, and satellite images (Corona KH-4 and WorldView-3). In their study, shoreline mapping was performed manually, and erosion rates were calculated using DSAS and the EPR index. Calculation of the uncertainty assessment was made considering three parameters: spatial resolution, the accuracy of georeferencing, and topography-induced uncertainty. The result of the study was that along the shoreline, coastal retreat was slow in some places and high in others. The high erosion in some sites may have been due to anthropogenic factors, such as the construction of gas facilities in the area. A year later, ref. [31] estimated coastal erosion using EO data (Landsat, ERS, Gaofen) for the Alaska and Eastern Siberia regions between 1974 and 2017. The shoreline was manually mapped, and erosion rates were derived by measuring the length between the baseline and waterline. The most extensive erosion occurred along the Alaskan coast, followed by that of the Eastern Siberian coast.

Ref. [44] examined the dynamics of a coastal field of the western Gydan Peninsula in Russia using GeoEye-1 and WorldView-1 images. To assess the coastline erosion, the shoreline was first surveyed using the manual method; then, the DSAS tool was used to observe the erosion. The analysis concluded that a strong retreat of the coast emerged due to anthropogenic effects, as the study area included new construction. This resulted in a suggestion of always taking into consideration the erosion rates in engineering and construction work, while at the same time taking appropriate measures for the shoreline. In the same year, ref. [45] studied shoreline changes using orthophoto aerial photographs and high-resolution satellite imagery (Pleiades) for the east coast of the Parry Peninsula, Canada. Like previous studies, the shoreline was manually delineated, and the DSAS tool was used to measure the erosion rate. This revealed that the area is characterized by increasing erosion compared to previous years. Uncertainty assessment was achieved using an equation in [38].

Ref. [46] investigated the transformation of the coastal landscape in the former Lake Davislaguna, Svalbard, Russia for the period 1990–2021. Aerial and satellite images (Landsat and Sentinel-2) were used. Thus, as in previous studies, the shoreline was delineated using manual visual interpretation; then, the retrieved satellite images were compared with old maps and archival material to determine the changes in the landscape. The study demonstrated that there was an accumulation of both the land and the lake. The authors attributed this most probably to the increase of temperature in the area, which led to the retreat of the landscape.

According to the studies reviewed above, especially in comparison to the prior time periods, there is an increase in the rate of erosion observed in the different areas of the coastal zone. The studies mainly investigated long-term changes in the coastal zone and concluded that erosion had clearly escalated. The rate of erosion is correlated to the occurrence of extreme weather conditions. In addition, the extent of the erosion is directly related to the geomorphology and lithology of the area. The shoreline mapping method can provide high levels of accuracy; it is therefore the most used method in studies overall. Most of the studies analyzed above did not implement detailed validation, since they are considered reference studies.

3.1.2. Automatic Computer-Assisted Interpretation

Automatic computer interpretation methods implemented in Arctic studies and analyzed below include the following groups of methods: (i) segmentation-based methods, (ii) classification-based methods, and (iii) hybrid methods.

Segmentation-Based Methods

Segmentation-based methods separate an image into discrete sections depending on properties such as texture, color information and geometric shapes. Each of these features show similarity or consistency in the same region. At this point, it is considered a crucial step for the end user to be able to distinguish various areas based on their differences. These methods are therefore applied based on thresholding techniques, edge detection, and region definition.

Ref. [10] examined for the first time the erodibility of permafrost areas in the Chukotka region, Russia, using archival, geodetic, and remote sensing (GeoEye) data. The use of GIS assisted in the process of shoreline extraction. Shoreline erosion rates were calculated for each period using computational operations. The findings showed that the rates were increased with respect to the previous years, which was a result of the lithological and morphological characteristics of the area.

A few years later, ref. [47] studied coastal dynamics in the Kara Sea, Russia, using multi-temporal EO data for the period 1964–2022. They used aerial and satellite images (CoronaKH-4, HexagonKH9-17, GeoEye-1, WorldView-2, PlanetScope, Jilin Gaofen-03, and ALOS PRIZM). An uncertainty assessment was performed for the images used by calculating the Root Mean Square Error (RMSE) of all points in the image. The shoreline extraction method was based on segmentation, and erosion rates were calculated using the DSAS tool by applying the EPR index. The coast was characterized by a slight increase in retreat due to the presence of waves and thermal energy.

Very recently, ref. [48] used Synthetic Aperture Radar (SAR) images to visualize shoreline changes on the Drew Point coast, Alaska. The shoreline extraction took place using an automated method, which was modelled using statistics. More specifically, a region-based method was used, which divided the shoreline into segments. The DSAS tool provided statistical weighted regression models to calculate the erosion rate of the shoreline, and through these, validation was performed. The findings show that there is continuous erosion, and the rate of shoreline retreat is increasing.

From the above, it can be concluded that a small number of segmentation-based studies have been implemented in examining the shoreline properties in Arctic regions. An observation of the results obtained from those studies indicates that there is an increase in coastal erosion rates, which is likely a result of the thermodynamics associated with climate change. The key advantages of this group of methods include their ease in implementation and their use independently of any type of EO dataset or a combination of EO datasets from different sensors.

Classification-Based Methods

Classification methods are implemented in areas where water features seem darker due to substantial absorption of a certain wavelength, making it possible to map shoreline

locations [49,50]. Classification-based methods rely on the assignment of different labels, based on the target attributes, and identify the boundary between the land and the sea area as the shoreline. Two subcategories are identified as classification methods: pixel-based and object-based methods [51,52].

Ref. [32] used high-resolution CubeSat PlanetScope satellite images to measure shoreline changes in lakes through an object-based classification method. The study was conducted for lakes in Canada and Alaska for the period May–October 2017. The method was evaluated through bootstrapping analyses of the training data and comparisons of the collected field measurements. The result of the study was a large-scale reduction in lake shorelines across a range of climatic, physiographic, and hydrologic terrain. However, flooding was observed in some locations.

Ref. [7] assessed coastal erosion in addition to shoreline mapping for areas in Canada and Russia. A novel approach was presented, where backscatter data from the Sentinel-1 (S1) SAR product was used as an input file to generate a shoreline product via the U-Net architecture, which is a deep learning (DL) technique. This product was used as a reference to quantify the rate of coastal erosion and accretion through Change Vector Analysis (CVA). The analysis was applied to areas of permafrost in the Arctic for the years 2017–2020. The results of the study indicated average to maximum erosion rates.

This group of methods is a powerful tool for quantifying coastal erosion and deposition rates in the Arctic. It should be noted that machine learning (ML) classification methods were used in quite a few of the published studies. This is largely due to the promising potential of those approaches in providing accurate results robustly, being able to be used with any type of EO dataset.

Hybrid Methods

Hybrid methods are understood as the combination of different techniques for coastline extraction. Over the years and on a global scale, numerous studies have used these methods to extract coastlines in different regions around the world [11,53,54].

Ref. [55] attempted to develop an efficient hybrid shoreline mapping method in the Tuktoyaktuk area of Canada using high-resolution satellite imagery from Pleiades. Thus, a classification approach was proposed that incorporated the segmented image method with semi-automatic land and water separation by calculating NDWI, based on texture analysis of Local Binary Pattern (LBP) and Random Forest (RF) classification. Each of the applicable methods was compared with results of the Maximum Likelihood Classification (MLC) method. The validation of the methods was evaluated using independent reference samples, and the producer, user, overall accuracy, overall disagreement allocation, and overall quantity disagreement were calculated. From the results, it was found that the hybrid method has the highest accuracy at 88% and is suitable to be applied to the extraction of Arctic coastlines.

Another study was conducted in [56] using a combination of threshold-based segmentation methods and classification methods. This study assessed the use of radiometric indices NDWI and NDSWI, machine learning models Random Forest (RF) and eXtreme Gradient Boosting (xgboost), and a deep learning approach comprising a modified U-Net architecture to map Arctic coastlines using high-resolution satellite data in Alaska. According to the findings, the U-Net model outperforms single-pixel models like the RF method.

Later, ref. [33] applied a hybrid method to derive the time series of shoreline shifts in Arctic Norway in 1984–2022. The authors developed a methodology combining classification methods (Random Forest algorithm) and threshold-based methods (NDWI algorithm). Satellite images (Landsat-5, Landsat-7, and Sentinel-2) were obtained through the Google Earth Engine (GEE) platform, and data fusion (including sensor fusion, algorithm fusion, and decision fusion) was applied to improve classification accuracy and processing efficiency. The image classification method considered the structure and spatial characteristics, while the threshold segmentation method was based on the spectral characteristics of the

water. In terms of validation, independent data were generated to assess the accuracy of land cover classification and shoreline extraction. The result of the study was an overall classification accuracy of over 99% and an average shoreline error distance of less than 15 m. Also, this process helped to provide information to identify shorelines that are vulnerable to coastal changes in the future. The authors of this study also noted that the automated process yielded better results compared to the manual visual interpretation of shoreline extraction.

All in all, from the above studies it is evidenced that only a small number of studies have so far been proposed in this category to study coastal properties in the Arctic. The use of hybrid methods allows capitalizing on the advantages of each of the techniques included in the synergy to improve prediction capability.

3.2. Approaches for Quantifying Coastal Vulnerability in Arctic Areas

Vulnerability is the degree to which a system is unable to cope with or vulnerable to the damage caused by climate change, including climate variability and coastal hazards, such as extreme storms and large waves, capable of causing coastal erosion [57]. Today, research on vulnerability has increased compared to earlier years, as the influence of anthropogenic factors on daily developments has increased tremendously [19,58]. More research is required on this issue to obtain appropriate management strategies and to develop better spatial distributions [59].

The vulnerability assessment aims to estimate the amount of damage to the community due to an extreme event, which may include material and physical damage and, in extreme situations, loss of human life [60,61]. The parameters that determine the vulnerability assessment are physical, ecological, and social. Remote sensing technologies are used for the data acquisition process. Especially in large-scale areas (e.g., Europe, USA), data collection is more effective when carried out by these techniques. However, there are cases that are characterized by the unavailability of data due to factors related to the operations of each satellite [58]. Most studies of coastal areas are related to risks associated with the sea level rise and ecosystem diversification due to climate change as well as their impacts in a socio-economic context [62]. According to the international literature, the vulnerability of coastal areas can be assessed in various ways, such as index-based methods, indicators, dynamic computer models (e.g., the Dynamic Interactive Vulnerability Assessment (DIVA) tool), GIS, visualization tools, vulnerability curves, and modelling tools [61]. The usage of indices as an assessment method used in surveys in the Arctic region is discussed below. It is thus possible to map the vulnerable places in the coastal areas of the Arctic zone and to identify the risk associated with shoreline change.

The index-based method is one of the most important methods for assessing vulnerability to erosion and flooding events as caused by SLR [63]. The main advantages of this method are speed, simplicity, and systematicity. In particular, the use of the index method can be described as a quantitative or semi-quantitative assessment derived through a combination of variables. Over the years, several studies have used this method to assess vulnerability [37,64,65]. A significant increase in vulnerability indices has been noted for specific coastal zones [66].

The "Coastal Vulnerability Index" is the most used method. The authors of [67] were the first to create an index to assess vulnerability, using seven different variables. Later, ref. [68] modified these parameters to analyze the effects of sea level rise on the United States. The modification led to the definition of the index with six different variables. A weighted factor is defined for each variable. The CVI index is computed by dividing the square root of the geometric mean or the product of specific variables by their sum and is expressed as follows [68]:

$$\mathrm{CVI} = \sqrt{\frac{a \times b \times c \times d \times e \times f}{6}} \quad (1)$$

where a = geomorphology, b = coastal slope, c = relative sea level rise rate, d = shoreline change rate, e = mean tide range, and f = mean wave height. The result of the index is quantified and classified into four categories that characterize vulnerability as low, moderate, high, and very high.

However, other composite vulnerability indicators and multi-scale indicators emerged from the evaluation of CVI development, such as the SVI (Socioeconomic Vulnerability Index), defined based on socio-economic variables, and the PVI (Physical Vulnerability Index), derived from physical variables [16]. The socio-economic parameters that contribute to the SVI are population, road networks, land uses, and infrastructure. Simultaneously, the analyzed physical parameters for the PVI index are coastal slope, coastline landforms, wave height, shoreline change rate, sea level rise, tidal data, and coastal elevation. Some other indices that have been used to assess vulnerability are the flow diagram-based risk zonation index, the analytical hierarchy process-based index, the coastal hazard index (CHI), the coastal sensitivity index (CSI), the Inundation Index, and Erosion Index.

Ref. [37], apart from shoreline extraction, carried out a vulnerability assessment using the CVI index in the Longyearbyen area, Svalbard, Norway, for the period 1990–2009. Equation (1) was used for calculation, where each of the six variables was calculated using a different methodology, either through field measurements or using existing databases. The result of the study was that most of the delineated shoreline sections showed low to moderate vulnerability. There were few areas where vulnerability was increased due to higher erosion. The authors attributed this to the limited sediment supply and the presence of the river system. In addition to this, human activities, such as the construction of new infrastructure, change the geomorphology of the area and lead to the alteration of the index results.

More recently, the authors of [65] developed the "Arctic Coastal Hazard Index (ACHI)" to evaluate the Arctic coast's vulnerability to permafrost thaw, coastal erosion, and flooding, particularly in Alaska. Thus, using the land settlement index, the coastal permafrost thaw potential (PTP) was quantified. First, the coastal hazard index (HI) was calculated based on previous approaches [69] to identify locations in danger of erosion and floods. The HI index is defined as the geometric mean of seven component factors:

$$\mathrm{HI} = \left(\left(\mathrm{R_{Habitats}} \mathrm{R_{ShorelineType}} \mathrm{R_{Relief}} \mathrm{R_{Wind}} \mathrm{R_{Waves}} \mathrm{R_{SurgePotential}} \mathrm{R_{SLR}} \right) \right) \Big/ 7 \quad (2)$$

where RHabitats = habitat type, RShorelineType = geomorphology type, RRelief = coastal relief, RWind = wind exposure, RWaves = wave exposure, RSurgePotential = wave potential andSLR = sea level rise potential.

Equation (2) was used to calculate the ACHI, which includes the permafrost thaw precipitation potential (PTP). Thus, the ACHI is expressed as follows:

$$\mathrm{ACHI} = \sqrt{\mathrm{HI} \times \mathrm{R_{PTP}}}, \quad (3)$$

where RPTP = permafrost thaw precipitation potential.

The ACHI results are classified into quartiles and divided into four categories representing the levels of coastal risk, characterized as follows: high, medium, low, and stable. The calculation of the above index was performed to test the risk of erosion in the coastal zone in the Alaska area for future scenarios up to 2060. The results led to the conclusion that the western coast of the region is classified as high risk, while the other areas are characterized by a moderate risk. The high degree of coastal risk is likely due to the geology and lithology of the coasts, as well as the likelihood of melting in these areas.

The existing method regarding the evaluation of the coastal vulnerability uses the computation of different indices based on the relevant parameters and the available data. While this method overall presets the values of the variables, which makes the process intricate, the CVI index can be easily understood by non-specialists. In the above studies, several regions are associated with a high risk of erosion due to geomorphological and

meteorological reasons. The results of the coastal vulnerability are visualized in maps using GIS. In this case, GIS is an irreplaceable tool, used to merge and analyze data as well as visualize the spatial distribution of hazards and vulnerability.

3.3. Software Tools for Shoreline Property Analysis in Arctic Regions

With the rising research interest in shoreline mapping, there has been significant development of the geoinformation tools used for automating shoreline mapping, which are suitable for studies conducted in the Arctic zone. These software tools are summarized in Table 2, and their functionalities relevant to coastline property estimation are briefly described below.

Table 2. A summary of software tools and their operational products for shoreline mapping.

Software Tools	Satellite Products	Programming Language	Access	References
DSAS (v6.0)	Applicable in any satellite data	ArcGIS add-on module	GitHub	[70]
CoastSat (v2.5)	Landsat 5,7,8 Sentinel-2	Python	GitHub	[71]
SAET (v1.0)	Landsat 8,9 Sentinel-2A, -2B	Python	GitHub Zenodo	[72]
CASSIE	Landsat 5,7,8 Sentinel-2	JavaScript	GitHub	[73]

3.3.1. Digital Shoreline Analysis System (DSAS)

The Digital Shoreline Analysis System (DSAS) tool is used to monitor shorelines (https://www.usgs.gov/centers/whcmsc/science/digital-shoreline-analysis-system-dsas, (accessed on 15 March 2024)). This tool was developed in recent years by the United Nations Geological Survey (USGS). Specifically, this tool is defined as follows [70]: The user sets a distance to the baseline, along the coast, at which vertical cross sections are generated. The distance between each cross-section point on the shoreline and the baseline is crucial in calculating changes in the shoreline. These changes are calculated either by distance measurements or by statistical calculations using data from the cross-sectional feature table in the cross-section file. DSAS can lead to the calculation of long-term and short-term changes as well as predictions of future shoreline changes. Regarding long-term and short-term shoreline changes, these are calculated using the following indicators:

- Shoreline Change Envelope (SCE)—the total change in position of the coastline under consideration is measured;
- Net Shoreline Movement (NSM)—determines the distance between the oldest and the newest coastline;
- End Point Rate (EPR)—is determined by the distance of shoreline movement over the study period;
- Linear Regression Rate (LRR)—identifies a statistical rate of change by fitting a least squares regression to all coastlines at a particular intersection;
- The DSAS tool determines the morphodynamical behavior of the shoreline and its displacement associated with the geometry of the coastal zone [74].

3.3.2. CoastSAT

This is a Python-based open-source software development tool (version 6). It is compatible with version 3.6 (or later). The developer of the CoastSat toolkit is Kilian Vos, and the year of its official release was 2018. Windows, Linux, and Mac are the systems accepted by CoastSat. This toolkit gives the user permission to obtain time series, for more than 30 years, on the position of the coastline on any sandy coastline according to the satellite images available worldwide. Figure 4 presents a graphical representation of the CoastSat methodology implementation steps.

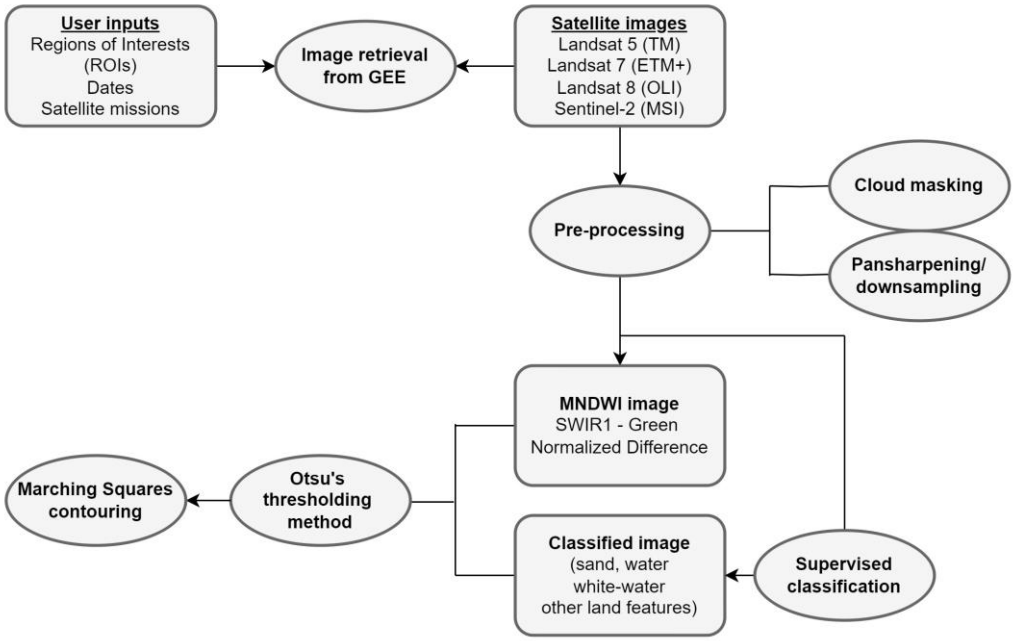

Figure 4. An illustration of the CoastSat tool workflow for shoreline position detection (credit: authors).

Satellite images are accessed through the Google Earth Engine (GEE) python Application Programming Interface (API). The functions of the CoastSat toolbox are outlined in the following stages: First, the images are retrieved from the GEE file. The second step is the pre-processing of the images, where processes such as cloud masking, downscaling, and sharpening take place. Continuing, the extraction of the analyzed coastlines into sub-pixels is performed. The last step is understood as the acquisition of time series at the shoreline position. The mapped shorelines are exported from the CoastSat toolbox in the ".geojson" file format, which allows them to be imported into GIS software.

The GEE API package can retrieve all Top-of-Atmosphere (TOA) reflectance images from the Landsat 5 (TM), Landsat 7 (EMT+), and Landsat 8 (OLI) Tier 1 collections, as well as from the Sentinel-2 (MSI) Level-1C mission products. TOA images are suitable for time series analysis as they are calibrated, and it is possible to compare images from different sensors at different times. However, before downloading the images, while they are still on the GEE platform, it is necessary to reduce their size. Thus, a number of regions of interest (known as ROIs) are defined for cropping the images. The cropped image consists of the three visible bands (R, G, B), the near infrared band (NIR), and the short wavelength infrared band (SWIR1), which are necessary to detect the coastline. In this way, the images are processed quickly, and the computer storage space is increased. Searching for large areas of interest can lead to a delay in processing.

In the pre-processing stage, the percentage of cloud cover occurring in the satellite image is calculated by applying a cloud mask. This percentage is obtained by defining a threshold, excluding all images exceeding this value. Continuing, resampling is performed, in which the spatial resolution of the image is improved so that all images have good spatial resolution. In this way, the coastline positioning is easier.

The next stage is the shoreline detection. On the pre-processed images, a reliable shoreline detection algorithm is applied to sub-pixel resolution from the CoastSat toolbox. When applying the algorithm, supervised image classification into four classes ("sand", "water", "white-water", "other land features") and sub-pixel resolution boundary segmentation is used. In supervised classification, a Neural Network classifier, called a "Multilayer Perceptron in scikit-learn", is used to characterize each pixel of each image [75]. At this

stage, the Modified Normalized Difference Water Index (MNDWI) is used in each of the classified images to detect the coastline. The MNDWI index is defined as follows:

$$MNDWI = \frac{SWIR1 - G}{SWIR1 + G} \quad (4)$$

where SWIR1 and G define the intensity of the pixel in the short-wavelength infrared band and in the green band, respectively. The values of the index range between −1 and 1. A histogram is then constructed, which separates the pixels of the "water" and "sand" class. By applying the "sand"/"water" quotient, the MNDWI index value is calculated using Otsu's thresholding algorithm [76].

Each mapped coastline is exported from the CoastSat toolbox in a user-defined spatial reference system, in the form of a 2D coordinate vector. This system is characterized by an accurate date and time of acquisition in Universal Time Coordinates (UTCs). Using an interactive graphical tool, quality control is performed, where each identified coastline is visualized and accepted or rejected through the CoastSat toolbox. By extracting the coastlines, the CoastSat toolbox helps to intersect the 2D coastlines with normal coastline cross sections. Then, along the cross sections, the time series of shoreline change are extracted. The cross sections are digitized either through an interactive ad hoc tool, manually by the user, or from a separate file imported from the cross-section coordinates.

A more detailed analysis of the CoastSat toolbox is provided in ref. [71]. The CoastSat toolkit is available via the link "https://github.com/kvos/CoastSat (accessed on 15 March 2024)" and features guided examples and a step-by-step README documentation file.

3.3.3. Shoreline Analysis and Extraction Tool (SAET)

This is a new open-source tool written in Python that uses optical images taken by Landsat 8 and 9 satellites and Sentinel-2 to achieve the automatic detection of changes in shoreline position during extreme events such as coastal storms. This tool was developed as part of the European Coastal Flood Awareness System project (ECFAS), which aims to be the first European service to predict, manage, and analyze coastal floods. It is designed as part of the Copernicus service to provide satellite-derived coastlines (SDS) in an automated system. However, this tool can be used locally by the user. [72] provide a more descriptive analysis on the SAET tool and its implementation. SAET is available for download from Zenodo.

For each action performed in this tool, it is necessary to take into account the requirements of the ECFAS project. These requirements include the use of the automatic function of the tool for the efficient acquisition of results. Also, to improve the definition of the coastline, it is important that the user can select multiple settings to ensure the process is flexible. Furthermore, data providers should have a direct interface from the SAET tool. For this reason, image management and acquisition platforms, such as GEE, are avoided.

The SAET tool receives as input files the satellite optical images of the Landsat 8 and 9, Sentinel-2A, and Sentinel-2B sensors and their ancillary data. The S2-A and S2-B images are obtained from the ESA server, while the L8 and L9 images are obtained from the USGS. Before the SAET tool can be launched, both data providers must give the requisite credentials. The USGS requires access to the machine-to-machine (M2M) application programming interface (API).

In the following, the steps of the tasks for running the SAET tool are described (Figure 5). Firstly, the images are downloaded from the respective servers, as mentioned above. The next step is the segmentation of the water–ground interface. This is achieved through different procedures, such as the K-means clustering technique or the combination of different zones. The water–terrain mask refinement is the third step in the process, where the SAET tool removes all shoreline pixels that are outside the beach areas or those in pixels classified as clouds. Then, shoreline sub-pixel extraction is performed, for which the basic algorithm, processed by the SHOREX system, is used [77,78]. The extracted coastlines are

stored in specific file formats and different geometries, such as ".shp" and ".json". Some auxiliary data are used by the SAET tool to improve its performance.

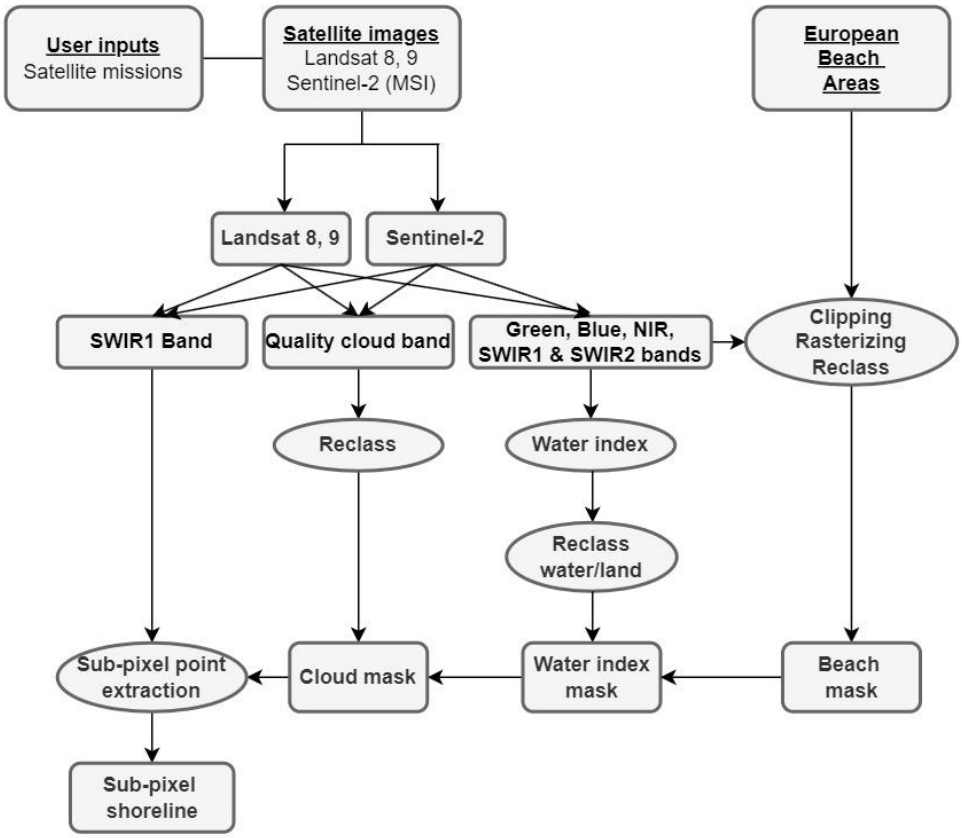

Figure 5. The schematic illustration of the SAET tool workflow for shoreline position detection (credit: authors).

The SAET tool works with a series of commands, followed by the appropriate parameters and a terminal window. These parameters concern the search, acquisition, and processing of images, the filters set, and the parameters used, to improve the exported product. The terminal window concerns an HTML file containing a preview of the images with all its main elements. Thus, the user will be able to select the most appropriate images. The local functionality of SAET will be able to assist in its use as an independent tool, thus helping to study the impacts of storm events.

3.3.4. Coastal Analyst System from Space Imagery Engine (CASSIE)

CASSIE is an open-source web-based tool that uses satellite images to analyze and map coastlines in any coastal area of the Earth (Figure 6). Its construction language is JavaScript, where it uses GEE API. Specifically, CASSIE uses the ShoreAnalyst module. The satellite imagery it uses is surface reflectance from the Landsat 5 (TM), Landsat 7 (EMT+) and Landsat 8 (OLI) Tier 1 collections, as well as Sentinel-2 (MSI) Level-1C products. As with CoastSat, this tool sets some ROIs to achieve image size reduction. When visualizing the images, only certain spectral bands—red, green, near infrared, and infrared—are made visible. CASSIE can be found at the following link https://cassiengine.org/ (accessed on 15 March 2024). Figure 6 shows a graphical representation of the CASSIE implementation steps, which are also briefly described below.

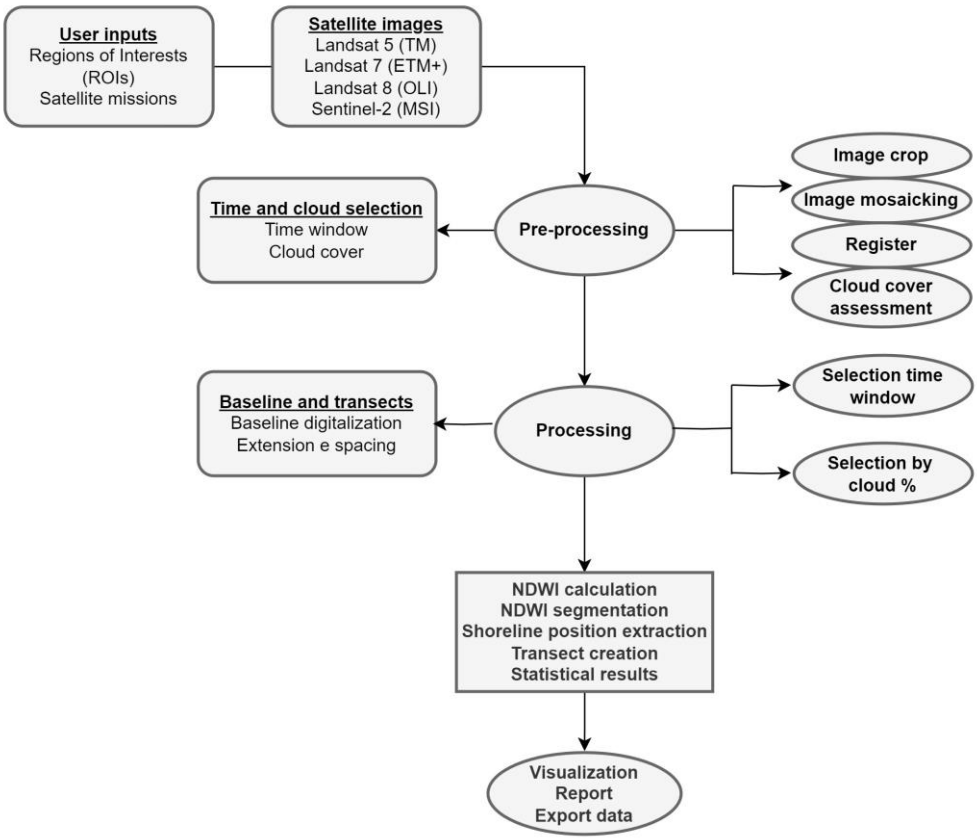

Figure 6. Workflow of CASSIE tool for shoreline mapping and analysis (credit: authors).

In the pre-processing stage, image mosaicking takes place, where spatial assembly of the image data takes place to produce a spatially continuous image. This is followed by the correction of the horizontal displacements between images, called image registration; the last stage of pre-processing is the calculation of the cloud cover. Also in the pre-processed images, an automatic shoreline detection algorithm is used by the CASSIE tool, with the help of the Normalized Difference Water Index (NDWI); it is applied as follows:

$$NDWI = \frac{(NIR - GREEN)}{(NIR + GREEN)} \quad (5)$$

where NIR and GREEN are the reflectance of the pixel in the near-infrared and green bands, respectively. From the results obtained, the lower NDWI (dark pixels) values define the low water content and therefore also the land class; the higher NDWI (light pixels) values define the high water content. The water class and the intermediate values belong to the intertidal ecosystem class. To properly establish the dry/water ratio, the tidal and water classes are grouped into a single class.

Continuing, CASSIE, for NDWI thresholding, uses the Otsu algorithm [76]. After applying the algorithm, a binary image is obtained, which is vectorized into polygons. The edge of the polygon that intersects the cross sections is defined as the coastline. The resulting coastline is smoothed using a 1D Gaussian smoothing filter.

Having completed the automatic shoreline extraction, a statistical analysis is implemented for everyone transect, based on the Digital Shoreline Analysis System—DSAS—software [79]. Once the statistical calculations are carried out, all the resulting transects and shorelines can be displayed either on a map or on a satellite image. The extracted information about the shorelines can be exported in the following file formats: .shp, .json, and .csv. Ref. [73] provides a more detailed analysis of the CASSIE tool.

3.4. Socio-Economic Studies and Coastal Properties

Global warming has resulted in significant effects on local and regional Arctic natural environments, infrastructure, and climate [80] with permafrost thawing having important socioeconomic impact globally [81]. Concerns arise over the monitoring of permafrost dynamics and the assessment of socioeconomic impacts and costs to local communities. In addition, as permafrost conditions retreat, the microbial decomposition of soil organic carbon is accelerating, with even more greenhouse gasses unleashed, exacerbating further climate change [82]. This is becoming even more urgent, as climate change has increased anthropogenic activity in the Arctic coastal region by 15% since 2000 [40]. Thus, obtaining a better understanding of the physical parameters that may have an impact on the Arctic climate and the potential socio-economic impacts of climate change in those environments is a key research priority. In this context, it is regarded today as a topic of key scientific priority and has made indispensable the development of methodologies and tools that can assist towards advancing our understanding in this direction. The latter has been highlighted as one of the most complex and emerging issues to be addressed today [83].

As evidenced from our literature review, most methods using EO focus on monitoring Arctic coastal dynamics under the physical processes' perspective. However, it is important to consider how these changes affect local and regional communities in both economic and social aspects. This is becoming important, as climate change has increased anthropogenic activity in the Arctic coastal region by 15% since 2000 [40]. Most studies following this approach focus on assessing the coastal vulnerability to a threat utilizing an index (see Section 3.3). However, as evidenced by the limited number of studies, their use remains underexplored. Apart from the use of vulnerability indices, there are several other approaches for linking EO-based products with socioeconomic studies. The authors of [84] studied changes in Impervious Surface Areas (ISAs) of a coastal area in Tromso region, Norway, over a timespan of 30 years, linking the increase in ISA with the population evolution. However, as reported by this study, the socioeconomic dataset availability, apart from the population, remained a significant challenge and limited the effort to achieve deeper insights.

Furthermore, particular focus has been given to assessing the vulnerability of Arctic coastal infrastructure to erosion. Permafrost thawing is a significant threat to Arctic infrastructure, with projections indicating that 30–50% of critical circumpolar infrastructure will be at high risk by 2050 [80]. Apart from the key production infrastructure, Arctic coastal cultural heritage sites are reported to be endangered across the circumpolar Arctic [85]. This has motivated several researchers in studying the exposure of cultural heritage sites to a variety of risks. The authors of [86] studied the risk exposure to floods of a potential cultural heritage site in Herschel Island, Yukon Territory, Canada, with their results demonstrating a rapid increase in the risk exposure. In [42], the authors used shoreline monitoring to evaluate coastal cultural heritage in Svalbard, Norway. Using drone imagery, morphological and sedimentological mapping was carried out to understand the changes occurring between the shoreline and the landscape. Their results showed that most of the heritage sites will disappear in the coming years.

As it becomes evident from the discussion above, there is a limited number of studies that try to link socioeconomic studies with EO-derived products. Factors such as data availability, spatial mismatch, and a lack of a standardized methodological framework for producing credible results heavily influence the further development of that pathway. However, there is an increasing need for addressing those challenges to fully reveal the implications of climate change for local and regional communities.

4. Relevant EO-Related Datasets, Platforms, and Projects Focusing on the Arctic

4.1. EO Datasets

As evidenced from the discussion so far, a variety of EO datasets have been used to study Arctic coastlines. Amongst the most frequently used EO-based datasets #used, most of the examined papers use optical satellite data from satellite sensors such as Landsat

archive (5, 8 and 9), Sentinel-2, MODIS imagery and orthophotos derived from either airplanes or drones [55]. Although there has been an abundance of optical sensors providing crucial insights over the area, optical data are severely impacted by cloud cover, which is considered high for the Arctic zone, thus hindering their widespread use. In this regard, SAR imagery has recently drawn much attention withSentinel-1 data has also been frequently used for coastline monitoring over the circumpolar Arctic [7]. New satellite missions focusing on the Arctic zone, such as CryoSat-2, are expected to provide data at an unprecedented scale, capturing the spatial and the temporal patterns of ice melting rates improving our understanding over the physical processes that take place in the area [87].

Furthermore, along with the increased volume of EO imagery itself, there has been a surge in derived datasets. A characteristic example of such a dataset is the Arctic Coastal Dynamics dataset, measuring erosion rates in the circumpolar Arctic zone [88]. In parallel, geoportals and WebGIS platforms hosting these datasets are being created, presenting the data while also providing to the user interaction capabilities. The National Snow and Ice Data Center (https://nsidc.org/home, accessed on 15 March 2024), a part of the Cooperative Institute for Research in Environmental Sciences (CIRES) at the University of Colorado Boulder, is an important distribution point for Arctic-related EO-based datasets. Another critical point of data distribution is the Norwegian Polar Institute (https://www.npolar.no/en/ accessed on 15 March 2024).

As new satellite missions are constantly launched with unprecedented capabilities in terms of spectral and spatial resolution, EO technology will be capable of providing more useful insights for the state of the Arctic zone, contributing to a much better understanding of Arctic coastal dynamics. However, the increased data volume and the lack of a single point of reference where datasets are organized are significant challenges. The EU, recognizing the key global role of permafrost changes in sustainable development and climate, has funded several EO- and cloud-based platforms (e.g., Permafrost CCI, Globpermafrost, APGC) for supporting Arctic-related research. However, information provided via the above-mentioned initiatives is currently dispersed through several web platforms, and open datasets provided by these platforms are available in various formats, making their use difficult and, in some cases, impractical.

4.2. Relevant EO Projects

The European Commission (EC) and other national/international funding bodies have funded several research projects that study Arctic coasts utilizing various geoinformation tools. Some examples of relevant research projects are the Arctic Coastal Dynamics (https://arcticcoast.info/, accessed on 15 March 2024), NUNATARYUK (https://nunataryuk.org/, accessed on 15 March 2024), and InteRFACE (https://arcticinterface.org/, accessed on 15 March 2024). One of the latest research projects funded by EC under the Marie Curie Staff Exchanges stream is EO-PERSIST (https://eo-persist.eu/) accessed on 15 March 2024, a research project aiming to develop a cloud-based remote sensing data system for promoting research and socioeconomic studies in Arctic environments. EU-funded projects contribute significantly to the study of Arctic coasts, producing datasets and studies that assist towards understanding the impact of climate change in these environments.

5. Scientific Challenges concerning the Use of EO/GIS in the Study of the Arctic Coast Properties

In summary, based on the findings of the present literature review, the main challenges regarding the different segments analyzed herein are the following:

(a) Regarding the coastal mapping detailed in Section 3.1:

- There is a notable challenge for finding suitable EO data for monitoring Arctic coasts. Optical data, the type of data most used in such studies, is severely limited by the increased cloud cover observed in the circumpolar Arctic and the coarse spatial resolution. Similarly, it is only from 2014 onwards that SAR imagery is available, mainly from the Sentinel-1 satellite.

(b) Concerning the methodologies employed for coastal mapping and erosion in Arctic regions, it is important to establish a common line or methodology protocol. Our review revealed that there is no specific action plan to follow in the case of studying coastline erosion. Regarding the coastal vulnerability detailed in Section 3.2:

- The coastal vulnerability in the Arctic is estimated using methods that account for factors such as habitat type, geomorphology, shoreline change rate, etc. Yet, in all the methods employed so far in the Arctic, these factors are weighed equally, which might not be the case in the real world. Consequently, further research is required in that direction, which will allow accounting for the weight of each factor in an objective way that will be user independent. In addition, a methodological framework should be developed towards assessing the accuracy of the derived vulnerability maps for the Arctic regions.
- Our review also evidenced that there is low awareness of the potential hazards and risks associated with coastal erosion, while as a result, there are limited strategies and area plans in place to proactively protect the high-risk regions.

(c) Regarding the software tools for shoreline property analysis detailed in Section 3.3:

- Although there is an abundance of software tools able to analyze shoreline characteristics, these tools are still based on simple techniques used to perform their analysis. State-of-the-art tools such as deep learning models, which outperform the thresholding techniques on which most software tools are based, have yet to be explored and potentially be integrated into these software tools. In addition, these software tools should include advanced capabilities, such as the ability to handle a big volume of data or performing computing processing in parallel processing, e.g., exploiting the power of high-performance computing.

(d) Regarding the socioeconomic studies detailed in Section 3.4:

- Socioeconomic studies that combine EO-based datasets with socioeconomic datasets are still rather limited for the Arctic region. The main reasons that hinder these approaches include the spatial mismatch between the EO-based indices and the socioeconomic datasets needed for these kinds of analysis. Evidently, future work is of paramount importance towards assessing the socioeconomic impacts of climate change in coastal areas exploiting geoinformation technologies.

(e) Regarding the relevant EO-related studies, platforms, and projects detailed in Section 4:

- The important contribution of geoinformation technologies such as EO and GIS has been recognized globally, e.g., by the fact that several EO- and cloud-based platforms (e.g., Permafrost CCI, Globpermafrost, APGC) are available supporting Arctic-related research. Yet, there is no single geoportal or WebGIS platform that collects and provides all the EO datasets for the Arctic in a systematic way, examining also the potential socio-economic impacts of climate change in Arctic coastal areas. Thus, there is an urgent need towards this directive.

6. Final Remarks

In the study, a systematic review was conducted on the different approaches for shoreline mapping and the analysis of coastal erosion and vulnerability in the Arctic region. A number of publications were selected and categorized in the following sectors: (a) shoreline extraction and erosion and (b) coastal vulnerability. The present study, to our knowledge, is the first of its kind in this domain and highlights the significant gap that exists due to the limited pool of studies on coastal monitoring and points out the necessity for further research. It focuses on and analyzes recent developments, identifies and confronts challenges, and provides direction for future pathways with a focus on exploiting both the EO dataset and state-of-the-art techniques.

The main conclusions from this review showed that the coastline of the Arctic zone has been constantly changing in recent years, and erosion rates are increasing. This is a result of both anthropogenic and natural factors, which need to be studied in parallel. Furthermore,

this study also demonstrates the importance and potential of geoinformation technologies overall and the high level of assistance they can provide in coastal detection and mapping. Finally, this study raises awareness with regard to the importance of monitoring coastal activity and erosion, in order to protect coastal areas and ensure a sustainable environment. Apart from adding more studies to the subject and continuing the research efforts, a game-changing process would be the development of a platform that allows the monitoring of coastal areas and assessment their vulnerability as well as the socioeconomic impact. In addition, these kinds of platforms will assist in the collection of data while helping to address emerging shoreline issues in a proactive way. This remains to be seen.

Author Contributions: Conceptualization, G.P.P., T.P., and S.E.D.; methodology, G.P.P., T.P., and S.E.D.; software, G.P.P., T.P., and S.E.D.; validation, T.P., G.P.P., and S.E.D.; formal analysis, T.P., G.P.P., and S.E.D.; data curation, G.P.P., T.P., and S.E.D.; writing—original draft preparation, T.P., G.P.P., and S.E.D.; writing—review and editing, T.P., G.P.P., and S.E.D.; visualization, T.P.; supervision, G.P.P.; funding acquisition, G.P.P.. All authors have read and agreed to the published version of the manuscript.

Funding: The present research study has been financially supported by the project "EO-PERSIST", funded by European Union's Horizon Europe Research and Innovation program HORIZON-MSCA-2021-SE-01-01 under grant agreement N. 101086386.

Data Availability Statement: Not applicable.

Acknowledgments: The authors wish to the thank the funding body for financially supporting the implementation of the present work and also the reviewers for their constructive feedback that helped improving the initially submitted manuscript.

Conflicts of Interest: The authors declare no conflicts of interest.

References

1. Malhi, Y.; Franklin, J.; Seddon, N.; Solan, M.; Turner, M.G.; Field, C.B.; Knowlton, N. Climate Change and Ecosystems: Threats, Opportunities and Solutions. *Philos. Trans. R. Soc. B* **2020**, *375*, 20190104. [CrossRef] [PubMed]
2. Nguyen, T.T.X.; Bonetti, J.; Rogers, K.; Woodroffe, C.D. Indicator-Based Assessment of Climate-Change Impacts on Coasts: A Review of Concepts, Methodological Approaches and Vulnerability Indices. *Ocean. Coast. Manag.* **2016**, *123*, 18–43. [CrossRef]
3. Bennett, N.; Blythe, J.; Tyler, S.; Ban, N.C. Communities and Change in the Anthropocene: Understanding Social-Ecological Vulnerability and Planning Adaptations to Multiple Interacting Exposures. *Reg. Environ. Change* **2016**, *16*, 907–926. [CrossRef]
4. Chen, C.; Bu, J.; Zhang, Y.; Zhuang, Y.; Chu, Y.; Hu, J.; Guo, B. The Application of the Tasseled Cap Transformation and Feature Knowledge for the Extraction of Coastline Information from Remote Sensing Images. *Adv. Space Res.* **2019**, *64*, 1780–1791. [CrossRef]
5. Yang, X.; Zhu, Z.; Qiu, S.; Kroeger, K.D.; Zhu, Z.; Covington, S. Detection and Characterization of Coastal Tidal Wetland Change in the Northeastern US Using Landsat Time Series. *Remote Sens. Environ.* **2022**, *276*, 113047. [CrossRef]
6. Frederick, J.; Thomas, M.A.; Bull, D.L.; Jones, C.; Roberts, J. *The Arctic Coastal Erosion Problem*; Sandia National Laboratories: Albuquerque, NM, USA, 2016. [CrossRef]
7. Philipp, M.; Dietz, A.J.; Ullmann, T.; Kuenzer, C. Automated Extraction of Annual Erosion Rates for Arctic Permafrost Coasts Using Sentinel-1, Deep Learning, and Change Vector Analysis. *Remote Sens.* **2022**, *14*, 3656. [CrossRef]
8. Jones, B.M.; Irrgang, A.M.; Farquharson, L.M.; Lantuit, H.; Whalen, D.; Ogorodov, S. The Sustained Transformation to a Warmer, Less Frozen and Biologically Changed Arctic Remains Clear. Arctic Report Card: Update for 2020. 2020. Available online: https://arctic.noaa.gov/Report-Card/Report-Card-2020/ArtMID/7975/ArticleID/904/Coastal-Permafrost-Erosion (accessed on 29 March 2024).
9. Jones, B.; Farquharson, L.M.; Baughman, C.A.; Buzard, R.M.; Arp, C.D.; Grosse, G.; Bull, D.L.; Günther, F.; Nitze, I.; Urban, F.E.; et al. A Decade of Remotely Sensed Observations Highlight Complex Processes Linked to Coastal Permafrost Bluff Erosion in the Arctic. *Environ. Res. Lett.* **2018**, *13*, 115001. [CrossRef]
10. Maslakov, A.; Kraev, G. Erodibility of Permafrost Exposures in the Coasts of Eastern Chukotka. *Polar Sci.* **2016**, *10*, 374–381. [CrossRef]
11. Liu, C.; Chang, J.; Chen, M.; Zhang, T. Dynamic Monitoring and Its Influencing Factors Analysis of Coastline in the Laizhou Bay since 1985. *J. Coast. Res.* **2020**, *105*, 18–22. [CrossRef]
12. Lantuit, H.; Overduin, P.; Wetterich, S. Recent Progress Regarding Permafrost Coasts. *Permafr. Periglac. Process.* **2013**, *24*, 120–130. [CrossRef]
13. Zhang, Y.; Hou, X. Characteristics of Coastline Changes on Southeast Asia Islands from 2000 to 2015. *Remote Sens.* **2020**, *12*, 519. [CrossRef]

14. Farquharson, L.M.; Mann, D.H.; Swanson, D.K.; Jones, B.; Buzard, R.M.; Jordan, J.W. Temporal and Spatial Variability in Coastline Response to Declining Sea-Ice in Northwest Alaska. *Mar. Geol.* **2018**, *404*, 71–83. [CrossRef]
15. De Serio, F.; Armenio, E.; Mossa, M.; Petrillo, A. How to Define Priorities in Coastal Vulnerability Assessment. *Geosciences* **2018**, *8*, 415. [CrossRef]
16. Rocha, C.; Antunes, C.; Catita, C. Coastal Indices to Assess Sea-Level Rise Impacts—A Brief Review of the Last Decade. *Ocean. Coast. Manag.* **2023**, *237*, 106536. [CrossRef]
17. Sun, W.; Chen, C.; Liu, W.; Yang, G.; Meng, X.; Wang, L.; Ren, K. Coastline Extraction Using Remote Sensing: A Review. *Gisci. Remote Sens.* **2023**, *60*, 2243671. [CrossRef]
18. El-Kafrawy, S.B.; Basheer, M.A.; Mohamed, H.M.; Naguib, D.M. Applications of Remote Sensing and GIS Techniques to Evaluate the Effectiveness of Coastal Structures along Burullus Headland-Eastern Nile Delta, Egypt. *Egypt. J. Remote Sens. Space Sci.* **2021**, *24*, 247–254. [CrossRef]
19. Noor, N.M.; Maulud, K.N.A. Coastal Vulnerability: A Brief Review on Integrated Assessment in Southeast Asia. *J. Mar. Sci. Eng.* **2022**, *10*, 595. [CrossRef]
20. Im, J. Earth Observations and Geographic Information Science for Sustainable Development Goals. *Gisci. Remote Sens.* **2020**, *57*, 591–592. [CrossRef]
21. Kouhgardi, E.; Hemati, M.; Shakerdargah, E.; Shiri, H.; Mahdianpari, M. Monitoring Shoreline and Land Use/Land Cover Changes in Sandbanks Provincial Park Using Remote Sensing and Climate Data. *Water* **2022**, *14*, 3593. [CrossRef]
22. Handiani, D.N.; Heriati, A.; Gunawan, W.A. Comparison of Coastal Vulnerability Assessment for Subang Regency in North Coast West Java-Indonesia. *Geomat. Nat. Hazards Risk* **2022**, *13*, 1178–1206. [CrossRef]
23. Ankrah, J.; Monteiro, A.; Madureira, H. Shoreline Change and Coastal Erosion in West Africa: A Systematic Review of Research Progress and Policy Recommendation. *Geosciences* **2023**, *13*, 59. [CrossRef]
24. Eliades, M.; Michaelides, S.; Evagorou, E.; Fotiou, K.; Fragkos, K.; Leventis, G.; Theocharidis, C.; Panagiotou, C.F.; Mavrovouniotis, M.; Neophytides, S.; et al. Earth Observation in the EMMENA Region: Scoping Review of Current Applications and Knowledge Gaps. *Remote Sens.* **2023**, *15*, 4202. [CrossRef]
25. Cavalli, R.M. Remote Data for Mapping and Monitoring Coastal Phenomena and Parameters: A Systematic Review. *Remote Sens.* **2024**, *16*, 446. [CrossRef]
26. Murray, J.; Adam, E.; Woodborne, S.; Miller, D.; Xulu, S.; Evans, M. Monitoring Shoreline Changes along the Southwestern Coast of South Africa from 1937 to 2020 Using Varied Remote Sensing Data and Approaches. *Remote Sens.* **2023**, *15*, 317. [CrossRef]
27. Duarte, C.R.; Miranda, F.; Landau, L.; Souto, M.V.S.; Sabadia, J.A.B.; Da Silva Neto, C.Â.; De Castro Rodrigues, L.I.; Damasceno, A.M. Short-Time Analysis of Shoreline Based on RapidEye Satellite Images in the Terminal Area of Pecém Port, Ceará, Brazil. *Int. J. Remote Sens.* **2018**, *39*, 4376–4389. [CrossRef]
28. Qiu, L.; Zhang, M.; Zhou, B.; Cui, Y.; Yu, Z.; Liu, T.; Wu, S. Economic and Ecological Trade-Offs of Coastal Reclamation in the Hangzhou Bay, China. *Ecol. Indic.* **2021**, *125*, 107477. [CrossRef]
29. Novikova, A.; Belova, N.; Baranskaya, A.; Aleksyutina, D.; Maslakov, A.; Zelenin, E.; Shabanova, N.; Ogorodov, S. Dynamics of Permafrost Coasts of Baydaratskaya Bay (Kara Sea) Based on Multi-Temporal Remote Sensing Data. *Remote Sens.* **2018**, *10*, 1481. [CrossRef]
30. Sinitsyn, A.; Guégan, E.; Shabanova, N.; Kokin, O.; Ogorodov, S. Fifty Four Years of Coastal Erosion and Hydrometeorological Parameters in the Varandey Region, Barents Sea. *Coast. Eng.* **2020**, *157*, 103610. [CrossRef]
31. Wang, J.; Li, D.; Cao, W.; Lou, X.; Shi, A.; Zhang, H. Remote Sensing Analysis of Erosion in Arctic Coastal Areas of Alaska and Eastern Siberia. *Remote Sens.* **2022**, *14*, 589. [CrossRef]
32. Cooley, S.W.; Smith, L.C.; Ryan, J.C.; Pitcher, L.H.; Pavelsky, T. Arctic—Boreal Lake Dynamics Revealed Using CubeSat Imagery. *Geophys. Res. Lett.* **2019**, *46*, 2111–2120. [CrossRef]
33. Nylén, T.N.; Gonzales-Inca, C.; Calle Navarro, M. Procedure for examining long-term Arctic shoreline displacement from multispectral satellite data. In Proceedings of the EGU General Assembly 2023, Vienna, Austria, 24–28 April 2023. EGU23-11651. [CrossRef]
34. Moussa, R.M.; Fogg, L.; Bertucci, F.; Calandra, M.; Collin, A.; Aubanel, A.; Polti, S.; Benet, A.; Salvat, B.; Galzin, R.; et al. Long-Term Coastline Monitoring on a Coral Reef Island (Moorea, French Polynesia). *Ocean. Coast. Manag.* **2019**, *180*, 104928. [CrossRef]
35. Lantuit, H.; Pollard, W.H. Fifty Years of Coastal Erosion and Retrogressive Thaw Slump Activity on Herschel Island, Southern Beaufort Sea, Yukon Territory, Canada. *Geomorphology* **2008**, *95*, 84–102. [CrossRef]
36. Zagórski, P. Shoreline Dynamics of Calypsostranda (NW Wedel Jarlsberg Land, Svalbard) during the Last Century. *Pol. Polar Res.* **2011**, *32*, 67–99. [CrossRef]
37. Jaskólski, M.; Pawłowski, Ł.; Strzelecki, M.C. High Arctic Coasts at Risk—The Case Study of Coastal Zone Development and Degradation Associated with Climate Changes and Multidirectional Human Impacts in Longyearbyen (Adventfjorden, Svalbard). *Land Degrad. Dev.* **2018**, *29*, 2514–2524. [CrossRef]
38. Irrgang, A.; Lantuit, H.; Manson, G.K.; Günther, F.; Grosse, G.; Overduin, P. Variability in Rates of Coastal Change along the Yukon Coast, 1951 to 2015. *J. Geophys. Res. Earth Surf.* **2018**, *123*, 779–800. [CrossRef]
39. Günther, F.; Overduin, P.P.; Sandakov, A.V.; Grosse, G.; Grigoriev, M.N. Short- and long-term thermo-erosion of ice-rich permafrost coasts in the Laptev Sea region. *Biogeosciences* **2013**, *10*, 4297–4318. [CrossRef]

40. Bartsch, A.; Ley, S.; Nitze, I.; Pointner, G.; Vieira, G. Feasibility Study for the Application of Synthetic Aperture Radar for Coastal Erosion Rate Quantification across the Arctic. *Front. Environ. Sci.* **2020**, *8*, 143. [CrossRef]
41. Zagórski, P.; Jarosz, K.; Superson, J. Integrated Assessment of Shoreline Change along the Calypsostranda (Svalbard) from Remote Sensing, Field Survey and GIS. *Mar. Geod.* **2020**, *43*, 433–471. [CrossRef]
42. Nicu, I.C.; Rubensdotter, L.; Stalsberg, K.; Nau, E. Coastal Erosion of Arctic Cultural Heritage in Danger: A Case Study from Svalbard, Norway. *Water* **2021**, *13*, 784. [CrossRef]
43. Novikova, A.; Vergun, A.; Zelenin, E.; Baranskaya, A.; Ogorodov, S. Determining Dynamics of the Kara Sea Coasts Using Remote Sensing and UAV Data: A Case Study. *Russ. J. Earth Sci.* **2021**, *21*, ES3004. [CrossRef]
44. Belova, N.; Ermolov, A.; Novikova, A.; Ogorodov, S.; Stanilovskaya, Y.V. Dynamics of Low-Lying Sandy Coast of the Gydan Peninsula, Kara Sea, Russia, Based on Multi-Temporal Remote Sensing Data. *Remote Sens.* **2022**, *15*, 48. [CrossRef]
45. Tanguy, R.; Whalen, D.; Prates, G.; Vieira, G. Shoreline Change Rates and Land to Sea Sediment and Soil Organic Carbon Transfer in Eastern Parry Peninsula from 1965 to 2020 (Amundsen Gulf, Canada). *Arct. Sci.* **2023**, *9*, 506–525. [CrossRef]
46. Ziaja, W.; Ostafin, K.; Maciejowski, W.; Kruse, F. Coastal Landscape Degradation and Disappearance of Davislaguna Lake, Sørkappland, Svalbard, 1900–2021. *Land Degrad. Dev.* **2023**, *34*, 4823–4832. [CrossRef]
47. Kazhukalo, G.; Novikova, A.; Shabanova, N.; Drugov, M.; Myslenkov, S.; Shabanov, P.; Belova, N.; Ogorodov, S. Coastal Dynamics at Kharasavey Key Site, Kara Sea, Based on Remote Sensing Data. *Remote Sens.* **2023**, *15*, 4199. [CrossRef]
48. Tsai, Y.-L. Monitoring Arctic Permafrost Coastal Erosion Dynamics Using a Multidecadal Cross-Mission SAR Dataset along an Alaskan Beaufort Sea Coastline. *Sci. Total Environ.* **2024**, *917*, 170389. [CrossRef] [PubMed]
49. Zhang, Y. Environmental Monitoring of Spatial-Temporal Changes Using Remote Sensing and GIS Techniques in the Abandoned Yellow River Delta Coast, China. *Int. J. Environ. Pollut.* **2011**, *45*, 327. [CrossRef]
50. Sekar, C.S.; Kankara, R.S.; Kalaivanan, P. Pixel-Based Classification Techniques for Automated Shoreline Extraction on Open Sandy Coast Using Different Optical Satellite Images. *Arab. J. Geosci.* **2022**, *15*, 939. [CrossRef]
51. Ghassemian, H. A Review of Remote Sensing Image Fusion Methods. *Inf. Fusion* **2016**, *32*, 75–89. [CrossRef]
52. Gašparović, M.; Jogun, T. The Effect of Fusing Sentinel-2 Bands on Land-Cover Classification. *Int. J. Remote Sens.* **2017**, *39*, 822–841. [CrossRef]
53. Yu, Y.; Zhang, Z.; Shokr, M.; Hui, F.; Cheng, X.; Chi, Z.; Heil, P.; Chen, Z. Automatically Extracted Antarctic Coastline Using Remotely-Sensed Data: An Update. *Remote Sens.* **2019**, *11*, 1844. [CrossRef]
54. De Vries, J.; Van Maanen, B.; Ruessink, G.; Verweij, P.A.; De Jong, S.M. Unmixing Water and Mud: Characterizing Diffuse Boundaries of Subtidal Mud Banks from Individual Satellite Observations. *Int. J. Appl. Earth Obs. Geoinf.* **2021**, *95*, 102252. [CrossRef]
55. Chen, Z.; Pasher, J.; Duffe, J.; Behnamian, A. Mapping Arctic Coastal Ecosystems with High Resolution Optical Satellite Imagery Using a Hybrid Classification Approach. *Can. J. Remote Sens.* **2017**, *43*, 513–527. [CrossRef]
56. Aryal, B.; Escarzaga, S.M.; Zesati, S.A.V.; Vélez-Reyes, M.; Fuentes, O.; Tweedie, C. Semi-Automated Semantic Segmentation of Arctic Shorelines Using Very High-Resolution Airborne Imagery, Spectral Indices and Weakly Supervised Machine Learning Approaches. *Remote Sens.* **2021**, *13*, 4572. [CrossRef]
57. IPCC. *Climate Change 2013—The Physical Science Basis. Contribution of Working Groups I, II and III to the Fifth Assessment Report of the Intergovernmental Panel on Climate Change, Intergovernmental Panel on Climate Change*; Climate Change 2014: Synthesis Report; Sydowed, I., Ed.; Cambridge University Press: Cambridge, UK, 2014.
58. Parthasarathy, K.S.S.; Deka, P.C. Remote sensing and GIS application in assessment of coastal vulnerability and shoreline changes: A review. *ISH J. Hydraul. Eng.* **2021**, *27*, 588–600. [CrossRef]
59. Silva, R.; Chávez, V.; Bouma, T.J.; Van Tussenbroek, B.I.; Arkema, K.K.; Martínez, M.L.; Oumeraci, H.; Heymans, J.J.; Osorio, A.F.; Mendoza, E.; et al. The Incorporation of Biophysical and Social Components in Coastal Management. *Estuaries Coasts* **2019**, *42*, 1695–1708. [CrossRef]
60. Ummenhofer, C.C.; Meehl, G.A. Extreme Weather and Climate Events with Ecological Relevance: A Review. *Philos. Trans. R. Soc. B* **2017**, *372*, 20160135. [CrossRef] [PubMed]
61. Cruz-Ramírez, C.J.; Chávez, V.; Silva, R.; Muñoz-Pérez, J.J.; Rivera-Arriaga, E. Coastal Management: A Review of Key Elements for Vulnerability Assessment. *J. Mar. Sci. Eng.* **2024**, *12*, 386. [CrossRef]
62. Balica, S.; Wright, N.; Van Der Meulen, F. A Flood Vulnerability Index for Coastal Cities and Its Use in Assessing Climate Change Impacts. *Nat. Hazards* **2012**, *64*, 73–105. [CrossRef]
63. Chakraborty, S. *Remote Sensing and GIS in Environmental Management*; Springer: Cham, Switzerland, 2021; pp. 185–220. [CrossRef]
64. Komi, A.; Petropoulos, A.; Evelpidou, N.; Πούλος, Σ.; Kapsimalis, V. Coastal Vulnerability Assessment for Future Sea Level Rise and a Comparative Study of Two Pocket Beaches in Seasonal Scale, IOS Island, Cyclades, Greece. *J. Mar. Sci. Eng.* **2022**, *10*, 1673. [CrossRef]
65. Wang, Z.; Xiao, M.; Nicolsky, D.; Romanovsky, V.E.; McComb, C.; Farquharson, L.M. Arctic Coastal Hazard Assessment Considering Permafrost Thaw Subsidence, Coastal Erosion, and Flooding. *Environ. Res. Lett.* **2023**, *18*, 104003. [CrossRef]
66. Saikrishnan, K.; KV, A.; Agilan, V. Coastal Vulnerability Assessment along the Coast of Kerala, India, Based on Physical, Geological, and Socio-Economic Parameters. *Mar. Geod.* **2024**, *47*, 119–149. [CrossRef]
67. Gornitz, V. Vulnerability of the East Coast, USA to future sea level rise. *J. Coast. Res.* **1990**, *9*, 201–237.

68. Thieler, E.R.; Hammar-Klose, E.S. *National Assessment of Coastal Vulnerability to Sea-Level Rise: Preliminary Results for the U.S. Atlantic Coast*; Open-file Report/1999; US Geological Survey: Reston, VA, USA, 1999. [CrossRef]
69. Arkema, K.K.; Guannel, G.; Verutes, G.M.; Wood, S.A.; Guerry, A.D.; Ruckelshaus, M.; Kareiva, P.; Lacayo, M.; Silver, J.M. Coastal Habitats Shield People and Property from Sea-Level Rise and Storms. *Nat. Clim. Change* **2013**, *3*, 913–918. [CrossRef]
70. Himmelstoss, E.A.; Henderson, R.E.; Kratzmann, M.G.; Farris, A.S. *Digital Shoreline Analysis System (DSAS) Version 5.0 User Guide*; Open-file Report/2018; US Geological Survey: Reston, VA, USA, 2018. [CrossRef]
71. Vos, K.; Splinter, K.D.; Harley, M.D.; Simmons, J.A.; Turner, I.L. CoastSat: A Google Earth Engine-Enabled Python Toolkit to Extract Shorelines from Publicly Available Satellite Imagery. *Environ. Model. Softw.* **2019**, *122*, 104528. [CrossRef]
72. Palomar-Vázquez, J.; Pardo-Pascual, J.E.; Almonacid-Caballer, J.; Cabezas-Rabadán, C. Shoreline Analysis and Extraction Tool (SAET): A New Tool for the Automatic Extraction of Satellite-Derived Shorelines with Subpixel Accuracy. *Remote Sens.* **2023**, *15*, 3198. [CrossRef]
73. Almeida, L.P.; De Oliveira, I.E.; Lyra, R.; Dazzi, R.L.S.; Martins, V.G.; Da Fontoura Klein, A.H. Coastal Analyst System from Space Imagery Engine (CASSIE): Shoreline Management Module. *Environ. Model. Softw.* **2021**, *140*, 105033. [CrossRef]
74. Moussaid, J.; Fora, A.A.; Zourarah, B.; Maanan, M.; Maanan, M. Using Automatic Computation to Analyze the Rate of Shoreline Change on the Kenitra Coast, Morocco. *Ocean. Eng.* **2015**, *102*, 71–77. [CrossRef]
75. Civco, D.L. Artificial neural networks for land-cover classification and mapping. *Int. J. Geogr. Inf. Syst.* **1993**, *7*, 173–186. [CrossRef]
76. Otsu, N. A Threshold Selection Method from Gray-Level Histograms. *IEEE Trans. Syst. Man Cybern.* **1979**, *9*, 62–66. [CrossRef]
77. Sánchez-García, E.; Palomar-Vázquez, J.; Pardo-Pascual, J.E.; Almonacid-Caballer, J.; Cabezas-Rabadán, C.; Gómez-Pujol, L. An Efficient Protocol for Accurate and Massive Shoreline Definition from Mid-Resolution Satellite Imagery. *Coast. Eng.* **2020**, *160*, 103732. [CrossRef]
78. Cabezas-Rabadán, C.; Pardo-Pascual, J.E.; Palomar-Vázquez, J. Characterizing the Relationship between the Sediment Grain Size and the Shoreline Variability Defined from Sentinel-2 Derived Shorelines. *Remote Sens.* **2021**, *13*, 2829. [CrossRef]
79. Thieler, E.R.; Himmelstoss, E.A.; Zichichi, J.L.; Ergul, A. Digital Shoreline Analysis System (DSAS) Version 4.0, an ArcGIS Extension for Calculating Shoreline Change. US Geological Survey Open-File Report 2008-1278. 2017. Available online: https://pubs.usgs.gov/publication/ofr20081278 (accessed on 26 May 2024).
80. Hjort, J.; Streletskiy, D.; Doré, G. Impacts of permafrost degradation on infrastructure. *Nat. Rev. Earth Environ.* **2022**, *3*, 24–38. [CrossRef]
81. Schuur, E.A.; McGuire, A.D.; Schädel, C.; Grosse, G.; Harden, J.W.; Hayes, D.J.; Hugelius, G.; Koven, C.D.; Kuhry, P.; Lawrence, D.M.; et al. Climate change and the permafrost carbon feedback. *Nature* **2015**, *520*, 171–179. [CrossRef] [PubMed]
82. Hugelius, G.; Strauss, J.; Zubrzycki, S.; Harden, J.W.; Schuur, E.A.G.; Ping, C.-L.; Schirrmeister, L.; Grosse, G.; Michaelson, G.J.; Koven, C.D.; et al. Estimated stocks of circumpolar permafrost carbon with quantified uncertainty ranges and identified data gaps. *Biogeosciences* **2014**, *11*, 6573–6593. [CrossRef]
83. European Commission. *An Integrated EU Policy for the Arctic, Opinion of the Committee on Foreign Affairs, 2016/17:UU6*; European Commission: Brussels, Belgium, 2017.
84. Dermosinoglou, A.; Detsikas, S.E.; Petropoulos, G.; Fratsea, L.M.; Papadopoulos, A. Multitemporal monitoring of Impervious Surface Areas (ISA) changes in an Arctic setting, using ML, Remote Sensing data and GEE, Google Earth Engine and Artificial Intelligence for Earth Observation Algorithms for Sustainable Applications. 2023. Available online: https://zenodo.org/records/10435903 (accessed on 26 May 2024).
85. Sesana, E.; Gagnon, A.S.; Ciantelli, C.; Cassar, J.A.; Hughes, J.J. Climate change impacts on cultural heritage: A literature review. *WIREs Clim. Change* **2021**, *12*, e710. [CrossRef]
86. Radosavljevic, B.; Lantuit, H.; Pollard, W. Erosion and Flooding—Threats to Coastal Infrastructure in the Arctic: A Case Study from Herschel Island, Yukon Territory, Canada. *Estuaries Coasts* **2016**, *39*, 900–915. [CrossRef]
87. Landy, J.C.; Dawson, G.J.; Tsamados, M. A year-round satellite sea-ice thickness record from CryoSat-2. *Nature* **2022**, *609*, 517–522. [CrossRef]
88. Lantuit, H.; Overduin, P.; Couture, N.; Wetterich, S.; Are, F.E.; Atkinson, D.E.; Brown, J.; Cherkashov, G.; Drozdov, D.; Forbes, D.L.; et al. The Arctic Coastal Dynamics Database: A New Classification Scheme and Statistics on Arctic Permafrost Coastlines. *Estuaries Coasts* **2012**, *35*, 383–400. [CrossRef]